Steel and Composite Structures, *Vol. 26, No. 4 (2018) 473-484*
DOI: https://doi.org/10.12989/scs.2018.26.4.473

Free vibration of cross-ply laminated plates based on higher-order shear deformation theory

Saira Javed [1], K.K. Viswanathan [*1,2], M.D. Nurul Izyan [1], Z.A. Aziz [1] and J.H. Lee [3]

[1] *UTM Centre for Industrial and Applied Mathematics (UTM-CIAM), Ibnu Sina Instituite for Scientific & Industrial Research, Universiti Teknologi Malaysia, 81310 Johor Bahru, Johor, Malaysia*
[2] *Kuwait College of Science and Technology, Doha District, Block 4, P.O. Box 27235, Safat 13133, Kuwait*
[3] *Department of Naval Architecture & Ocean Engineering, Inha University, 100 inharo, Nam-gu Incheon 22212, South Korea*

(*Received August 11, 2017, Revised November 15, 2017, Accepted December 14, 2017*)

Abstract. Free vibration of cross-ply laminated plates using a higher-order shear deformation theory is studied. The arbitrary number of layers is oriented in symmetric and anti-symmetric manners. The plate kinematics are based on higher-order shear deformation theory (HSDT) and the vibrational behaviour of multi-layered plates are analysed under simply supported boundary conditions. The differential equations are obtained in terms of displacement and rotational functions by substituting the stress-strain relations and strain-displacement relations in the governing equations and separable method is adopted for these functions to get a set of ordinary differential equations in term of single variable, which are coupled. These displacement and rotational functions are approximated using cubic and quantic splines which results in to the system of algebraic equations with unknown spline coefficients. Incurring the boundary conditions with the algebraic equations, a generalized eigen value problem is obtained. This eigen value problem is solved numerically to find the eigen frequency parameter and associated eigenvectors which are the spline coefficients.The material properties of Kevlar-49/epoxy, Graphite/Epoxy and E-glass epoxy are used to show the parametric effects of the plates aspect ratio, side-to-thickness ratio, stacking sequence, number of lamina and ply orientations on the frequency parameter of the plate. The current results are verified with those results obtained in the previous work and the new results are presented in tables and graphs.

Keywords: free vibration; higher-order theory; spline; composite plates; cross-ply

1. Introduction

Composite laminate shows a better results using different material properties as compared to a single layer and homogenous material structures owing to the large number of parameters associated with manufacturing processes. The aim of the designer is to control unwarranted vibrations, which leads to the failure of the structure. Composite materials have the ability to tailor the mechanical properties. Moreover, composites offer high stiffness to weight ratio, strength to weight ratios, better temperature resistance and shock absorbing characteristics than homogeneous materials. The use of the lamination leads to the structures which have maximum reliability and minimum weight. Also that the laminated composite plates exhibit larger through-thickness effects than the structures made of homogeneous materials, which means that higher-order shear deformation theories are often required for these structures.

A large number of theories have been proposed by different researchers which generally differ in the inclusion of the shear deformation and rotary inertia in their formulations. The classical theory is based on the Love-Kirchhoff assumption. In this theory, the straight lines normal to the undeformed and deformed mid-plane remains straight and normal and do not undergo stretching in the thickness direction. These assumptions imply the vanishing of the transverse shear and transverse normal strains. This theory accurately measures the stress analysis of thin composites plates. This theory is not suitable for thick laminated plates since it has over prediction in natural frequencies (Noor *et al*. 1996, Vinson 2001). In order to study the relatively thick plates, the effect of shear deformation should be taken in to account. Reissner (1945) first introduced the transverse shear deformation on analysing the bending of elastic plates and then Mindlin (1951) studied the influence of rotary inertia and shear on flexural motions of isotropic elastic plates. Yang *et al*. (1966) included transverse shear deformation and rotatory inertia in their study. According to the first-order shear deformation theory (FSDT), there is a state of constant shear strain through the thickness of the plate (transverse shear strain). However, according to the 3D elasticity theory, the shear strains vary at least quadratically through the thickness (transverse shear strain). So, the shear correction factors were introduce to correct the discrepancy in the shear forces of FSDT and 3D elasticity theory (Pai 1995, Pai and Schulz 1999). The value of the shear correction factors depends on the lamination properties, stacking sequence of layers, geometry and boundary conditions (Mackerle 2002, Yang *et al*. 2000). Moreover, a

*Corresponding author, Associate Professor,
E-mail: visu20@yahoo.com; k.viswanathan@kcst.edu.kw

ISSN: 1229-9367 (Print), 1598-6233 (Online)

number of higher-order plate theories were developed to evaluate the transverse shear stresses accurately which effectively exists in thick plates. In higher-order plate theories the displacements are expanded up to any desired degree in terms of the thickness coordinates (Noor *et al*. 1996, Vinson 2001). In the third-order plate theory the in plane-displacements are expanded up to the cubic term in the thickness coordinates to have a quadratic variation of transverse shear strains and transverse shear stresses through the plate thickness. This avoids the need for a shear correction coefficient (Reddy 2006). The third-order plate TSDT theory of Reddy is widely used because of the efficiency of transverse shear stresses.

Free and forced vibration of anti-symmetric plates was studied by Khdeir (2001). Free vibration of rectangular and annular plates were analysed using the spectral method (Ma'en and Butcher 2012). Saha *et al*. (2004) used the variational method to analyse the large amplitude free vibration of square plates for different boundary conditions. Bai and Chen (2013) found the free vibration solution of rectangular plates using the symplectic eigen function expansion approach. Pekovic *et al*. (2014) studied the bending analysis of composite plates under higher-order shear deformation theory. 2-D higher-order theory was used by Matsunaga (2008) to analyse the free vibration and stability of functionally graded plates. A new higher-order shear deformation theory was used to analyse the vibration of sandwich and composite laminated plates and shells (Mantari *et al*. 2011, 2012). Recently, Mantari and Granados (2015) examined the thermoelastic analysis of sandwich plates using the quasi 3-D hybrid type HSDT. Static inconsistencies of beams, plates and shells were investigated using higher-order shear deformation theory by Groh and Weaver (2015). Phung-Van *et al*. (2015a) analysed cell-based three-node Mindlin plates using C^0-type higher-order shear deformation for geometrically nonlinear analysis of composite plates. In another paper Phung-Van *et al*. (2015b) analysed the composite plates having piezoelectric sensors and actuators using HSDT. Thai *et al*. (2015) studied the isogeometric analysis of composite plates using HSDT. Smooth discrete shear gap method using C^0-type higher-order shear deformation theory for analysing the laminated plates were studied by Tran *et al*. (2013). Zhen and Wanji (2006) investigated a free vibration of laminated and sandwich plates using global-local higher-order shear deformation theory. Reddy's higher-order theory was used to examine the free vibration of composite sandwich plates (Nayak *et al*. 2002). Kant and Swaminathan (2001a, b, 2002) used refined higher-order shear deformation theory to analyse the multilayer plates. Composite plates were analysed using multiquadric radial basis function under higher-order shear deformation theory (Ferreira *et al*. 2003). Recently, Neves *et al*. (2013) investigated the static, free and buckling analysis of plates using quasi 3-D higher-order shear deformation theory. Cho and Parmerter (1993) studied the general lamination configuration using higher-order composite plate theory. A C^0 finite element formulation was used to analyse the laminated beams by Iurlaro *et al*. (2015). Karttunen and von Hertzen (2015) used an exact theory to study a linearly elastic beams. Zeroth-order shear deformation micro-mechanical model was used to analyse composite plates by Lee (2013). Rajagopal and Hodges (2015) examined the plates of variable thickness using variationally asymptotic analysis method. The spline method was used by Viswanathan *et al*. (2015a, b, c) and Viswanathan and Javed (2016) to solve the free vibrational problems of conical shells, cylindrical shells and annular circular plates using first order shear deformation theory. Further, Javed *et al*. (2016) analysed the free vibration of antisymmetric angle-ply plates using first-order shear deformation theory. A higher order shear deformation theory was used by Sheikh and Chakrabarti (2003) in studying the composite plates. In addition, Nguyen *et al*. (2016) applied higher order shear deformation theories for laminated composite plates using unified approach. Furthermore, Nguyen *et al*. (2017) investigated isotropic and functionally graded material plates using the generalized formulation of three-variable plate theory. Singh and Singh (2017) used higher order shear deformation theory for free vibration and buckling analysis of laminated and braided composite plates.

This paper intends to investigate the free vibration of symmetric and anti-symmetric cross-ply laminated plates using higher-order shear deformation theory and applying spline approximation technique. The plate kinematics is based on the third-order shear deformation theory (TSDT).

In Section 2, the problem is formulated to obtain a coupled differential equations in terms of displacement functions using the stress-strain relation and strain-displacement relations. In sub Section 2.3, the displacement and rotational functions are approximated using cubic and quantic splines. Collocation procedure is adopted with these splines to yield a set of field equations. Along with the equations of simply supported boundary conditions the set of field equations become a system of simultaneous algebraic equations on the assumed spline coefficients as a variable. Then the problem is solved using eigensolution technique to obtain the frequency parameters and the corresponding eigenvectors, which are the spline coefficients from which the mode shapes can be constructed. Section 3, shows the results of the frequency parameters which are obtained with respect to the plate aspect ratio, side-to-thickness ratio, ply angles, number of lamina with different material properties The results are presented in graphs and tables.

2. Formulation

The displacement field considered according to third-order shear deformation theory (Reddy 2006)

$$\begin{aligned} u(x,y,z,t) &= u_0(x,y,t) + z\phi_x(x,y,t) \\ &-\frac{4z^3}{3h^2}\left(\phi_x + \frac{\partial w_0}{\partial x}\right), \\ v(x,y,z,t) &= v_0(x,y,t) + z\phi_y(x,y,t) \\ &-\frac{4z^3}{3h^2}\left(\phi_y + \frac{\partial w_0}{\partial y}\right), \\ w(x,y,z,t) &= w_0(x,y,t), \end{aligned} \tag{1}$$

where u, v and w are the displacement components in the x, y and z directions respectively, u_0 and v_0 and w_0 are the in-plane displacements of the middle plane and ϕ_x and ϕ_y are the shear rotations of any point on the middle surface of the plate and h is the thickness of the plate.

2.1 Kinematics

In-plane strains are defined as

$$\varepsilon=\begin{Bmatrix}\varepsilon_x\\ \varepsilon_y\\ \gamma_{xy}\end{Bmatrix},\qquad \varepsilon=\varepsilon^0+z\varepsilon^1+z^3\varepsilon^3 \tag{2}$$

where

$$\varepsilon^0=\begin{Bmatrix}\varepsilon_x^0\\ \varepsilon_y^0\\ \gamma_{xy}^0\end{Bmatrix}=\begin{Bmatrix}\dfrac{\partial u_0}{\partial x}\\ \dfrac{\partial v_0}{\partial y}\\ \dfrac{\partial u_0}{\partial y}+\dfrac{\partial v_0}{\partial x}\end{Bmatrix},\varepsilon^1=\begin{Bmatrix}\varepsilon_x^1\\ \varepsilon_y^1\\ \gamma_{xy}^1\end{Bmatrix}=\begin{Bmatrix}\dfrac{\partial \phi_x}{\partial x}\\ \dfrac{\partial \phi_y}{\partial y}\\ \dfrac{\partial \phi_x}{\partial y}+\dfrac{\partial \phi_y}{\partial x}\end{Bmatrix},$$

$$\varepsilon^3=\begin{Bmatrix}\varepsilon_x^3\\ \varepsilon_y^3\\ \gamma_{xy}^3\end{Bmatrix}=\left(-\frac{4}{3h^2}\right)\begin{Bmatrix}\dfrac{\partial \phi_x}{\partial x}+\dfrac{\partial^2 w_0}{\partial x^2}\\ \dfrac{\partial \phi_y}{\partial y}+\dfrac{\partial^2 w_0}{\partial y^2}\\ \dfrac{\partial \phi_x}{\partial y}+\dfrac{\partial \phi_y}{\partial x}+2\dfrac{\partial^2 w_0}{\partial x\partial y}\end{Bmatrix},$$

and the shear strain components are defined as

$$\gamma=\begin{Bmatrix}\gamma_{yz}\\ \gamma_{xz}\end{Bmatrix},\qquad \gamma=\gamma^0+z^2\gamma^2 \tag{3}$$

where

$$\gamma^0=\begin{Bmatrix}\gamma_{yz}^0\\ \gamma_{xz}^0\end{Bmatrix}=\begin{Bmatrix}\phi_y+\dfrac{\partial w_0}{\partial y}\\ \phi_x+\dfrac{\partial w_0}{\partial x}\end{Bmatrix}$$

$$\gamma^2=\begin{Bmatrix}\gamma_{yz}^2\\ \gamma_{xz}^2\end{Bmatrix}=\left(-\frac{4}{h^2}\right)\begin{Bmatrix}\phi_y+\dfrac{\partial w_0}{\partial y}\\ \phi_x+\dfrac{\partial w_0}{\partial x}\end{Bmatrix}.$$

2.2 Constitutive equations

The stress-strain relations for the k-th layer, after neglecting transverse normal strain and stress, are of the form

$$\begin{pmatrix}\sigma_x^{(k)}\\ \sigma_y^{(k)}\\ \sigma_{xy}^{(k)}\\ \tau_{yz}^{(k)}\\ \tau_{xz}^{(k)}\end{pmatrix}=\begin{pmatrix}C_{11}^{(k)} & C_{12}^{(k)} & C_{16}^{(k)} & 0 & 0\\ C_{12}^{(k)} & C_{22}^{(k)} & C_{26}^{(k)} & 0 & 0\\ C_{16}^{(k)} & C_{26}^{(k)} & C_{66}^{(k)} & 0 & 0\\ 0 & 0 & 0 & C_{44}^{(k)} & C_{45}^{(k)}\\ 0 & 0 & 0 & C_{45}^{(k)} & C_{55}^{(k)}\end{pmatrix}\begin{pmatrix}\varepsilon_x^{(k)}\\ \varepsilon_y^{(k)}\\ \gamma_{xy}^{(k)}\\ \gamma_{yz}^{(k)}\\ \gamma_{xz}^{(k)}\end{pmatrix}. \tag{4}$$

When the materials are oriented at an angle θ with the x-axis, the transformed stress-strain relations are

$$\begin{pmatrix}\sigma_x^{(k)}\\ \sigma_y^{(k)}\\ \sigma_{xy}^{(k)}\\ \tau_{yz}^{(k)}\\ \tau_{xz}^{(k)}\end{pmatrix}=\begin{pmatrix}Q_{11}^{(k)} & Q_{12}^{(k)} & Q_{16}^{(k)} & 0 & 0\\ Q_{12}^{(k)} & Q_{22}^{(k)} & Q_{26}^{(k)} & 0 & 0\\ Q_{16}^{(k)} & Q_{26}^{(k)} & Q_{66}^{(k)} & 0 & 0\\ 0 & 0 & 0 & Q_{44}^{(k)} & Q_{45}^{(k)}\\ 0 & 0 & 0 & Q_{45}^{(k)} & Q_{55}^{(k)}\end{pmatrix}\begin{pmatrix}\varepsilon_x^{(k)}\\ \varepsilon_y^{(k)}\\ \gamma_{xy}^{(k)}\\ \gamma_{yz}^{(k)}\\ \gamma_{xz}^{(k)}\end{pmatrix} \tag{5}$$

where $Q_{ij}^{(k)}$, as functions of $C_{ij}^{(k)}$ are fully furnished in Viswanathan and Lee (2007).

The stress resultants are defined as

$$\begin{Bmatrix}N\\ M\\ P\end{Bmatrix}=\int_{-h/2}^{h/2}\sigma\begin{Bmatrix}1\\ z\\ z^3\end{Bmatrix}dz,\begin{Bmatrix}Q\\ R\end{Bmatrix}=\int_{-h/2}^{h/2}\tau\begin{Bmatrix}1\\ z^2\end{Bmatrix}dz, \tag{6}$$

where N, M and Q are stress, moment and shear resultants respectively. P and R denote the higher-order stress resultants.

The stress-strain relations are obtained as follows.

$$\begin{pmatrix}N\\ M\\ P\\ Q\\ R\end{pmatrix}=\begin{pmatrix}A & B & E & 0 & 0\\ B & D & F & 0 & 0\\ E & F & H & 0 & 0\\ 0 & 0 & 0 & A' & D'\\ 0 & 0 & 0 & D' & F'\end{pmatrix}\begin{pmatrix}\varepsilon^0\\ \varepsilon^1\\ \varepsilon^3\\ \gamma^0\\ \gamma^2\end{pmatrix} \tag{7}$$

Stiffness coefficients are defined as

$$\begin{aligned}A_{ij}&=\sum_k \bar{Q}_{ij}^{(k)}(z_k-z_{k-1})\\ B_{ij}&=\frac{1}{2}\sum_k \bar{Q}_{ij}^{(k)}(z^2{}_k-z^2{}_{k-1})\\ D_{ij}&=\frac{1}{3}\sum_k \bar{Q}_{ij}^{(k)}(z^3{}_k-z^3{}_{k-1})\\ E_{ij}&=\frac{1}{4}\sum_k \bar{Q}_{ij}^{(k)}(z^4{}_k-z^4{}_{k-1})\\ F_{ij}&=\frac{1}{5}\sum_k \bar{Q}_{ij}^{(k)}(z^5{}_k-z^5{}_{k-1})\\ H_{ij}&=\frac{1}{7}\sum_k \bar{Q}_{ij}^{(k)}(z^7{}_k-z^7{}_{k-1})\end{aligned} \tag{8}$$

for $i, j = 1, 2, 6,$

$$\begin{aligned}A'_{ij}&=\sum_k \bar{Q}_{ij}^{(k)}(z_k-z_{k-1})\\ D'_{ij}&=\frac{1}{3}\sum_k \bar{Q}_{ij}^{(k)}(z^3{}_k-z^3{}_{k-1})\\ F'_{ij}&=\frac{1}{5}\sum_k \bar{Q}_{ij}^{(k)}(z^5{}_k-z^5{}_{k-1})\end{aligned}$$

for $i, j = 4, 5,$

where the elastic coefficients A_{ij}, B_{ij} and D_{ij} (extensional, bending-extensional coupling and bending stiffness) and E_{ij},

F_{ij} and H_{ij} are the higher-order stiffness coefficients.

The equilibrium equations considered are as follows

$$\begin{aligned}
&\frac{\partial N_x}{\partial x}+\frac{\partial N_{xy}}{\partial y}=I_0\frac{\partial^2 u}{\partial t^2},\\
&\frac{\partial N_{xy}}{\partial x}+\frac{\partial N_y}{\partial y}+=I_0\frac{\partial^2 v}{\partial t^2},\\
&\frac{\partial \bar{Q}_x}{\partial x}+\frac{\partial \bar{Q}_y}{\partial y}+c_1\left(\frac{\partial^2 P_x}{\partial x^2}+2\frac{\partial^2 P_{xy}}{\partial x\partial y}+\frac{\partial^2 P_y}{\partial y^2}\right)=I_0\frac{\partial^2 w}{\partial t^2}\\
&-c_1^2 I_6\left(\frac{\partial^4 w_0}{\partial x^2\partial t^2}+\frac{\partial^4 w_0}{\partial y^2\partial t^2}\right)+c_1 J_4\left(\frac{\partial^3 \phi_x}{\partial x\partial t^2}+\frac{\partial^3 \phi_y}{\partial y\partial t^2}\right),\\
&\frac{\partial \bar{M}_x}{\partial x}+\frac{\partial \bar{M}_{xy}}{\partial y}-\bar{Q}_x=K_2\frac{\partial^2 \phi_x}{\partial t^2}-c_1 J_4\frac{\partial^3 w}{\partial x\partial t^2},\\
&\frac{\partial \bar{M}_{xy}}{\partial x}+\frac{\partial \bar{M}_y}{\partial y}-\bar{Q}_y=K_2\frac{\partial^2 \phi_y}{\partial t^2}-c_1 J_4\frac{\partial^3 w}{\partial x\partial t^2},
\end{aligned} \tag{9}$$

where $I_i=\int_z \rho^{(k)}(z)^i dz$ $(i=0,2,4,6)$ and ρ is the material density of the k-th layer and

$$\begin{aligned}
&\bar{M}_x=M_x-c_1P_x\ ,\ \bar{M}_y=M_y-c_1P_y\\
&\bar{M}_{xy}=M_{xy}-c_1P_{xy}\ ,\ \bar{Q}_x=Q_x-c_2R_x\\
&\bar{Q}_y=Q_y-c_2R_y\ ,\ J_i=I_i-c_1I_{i+2}\ ,\\
&K_2=I_2-2c_1I_4+c_1^2I_6.
\end{aligned}$$

The displacements and rotational functions are assumed in the separable form for cross-ply plates, which satisfies the simply-supported boundary conditions along the y- axis.

$$\begin{aligned}
u(x,y)&=U(x)\sin\frac{n\pi y}{b}\,e^{i\omega t}\\
v(x,y)&=V(x)\cos\frac{n\pi y}{b}e^{i\omega t}\\
w(x,y)&=W(x)\sin\frac{n\pi y}{b}e^{i\omega t}\\
\phi_x(x,y)&=\Phi_x(x)\sin\frac{n\pi y}{b}e^{i\omega t}\\
\phi_y(x,y)&=\Phi_y(x)\cos\frac{n\pi y}{b}e^{i\omega t}
\end{aligned} \tag{10}$$

The non-dimensional parameters introduced are as follows, where $\lambda=\omega a\sqrt{\frac{I_0}{A_{11}}}$ is a frequency parameter, $\delta_k=\frac{h_k}{h}$ is the relative layer thickness of the k-th layer, $\phi=\frac{a}{b}$ is the aspect ratio, $X=\frac{x}{a}$ is a distance co-ordinate, and $H=\frac{a}{h}$ is the side-to-thickness ratio.

Using Eq. (11) and introducing non-dimensional parameters in Eq. (10) the modified equation in the matrix form is obtained as

$$\begin{bmatrix}
L_{11}&L_{12}&L_{13}&L_{14}&L_{15}\\
L_{21}&L_{22}&L_{23}&L_{24}&L_{25}\\
L_{31}&L_{32}&L_{33}&L_{34}&L_{35}\\
L_{41}&L_{42}&L_{43}&L_{44}&L_{45}\\
L_{51}&L_{52}&L_{53}&L_{54}&L_{55}
\end{bmatrix}\begin{Bmatrix}U\\V\\W\\\Phi_X\\\Phi_Y\end{Bmatrix}=\begin{Bmatrix}0\\0\\0\\0\\0\end{Bmatrix}, \tag{11}$$

where

$$\begin{aligned}
&L_{11}=\frac{d^2}{dX^2}-s_{10}\beta^2+\lambda^2,\qquad L_{12}=-(s_2+s_{10})\beta\frac{d}{dX}\\
&L_{13}=-s_{17}c_1\frac{d^3}{dX^3}+(s_{18}c_1+2s_{26}c_1)\beta^2\frac{d}{dX}\\
&L_{14}=(s_4-s_{17}c_1)\frac{d^2}{dX^2}-(s_{11}-s_{26}c_1)\beta^2\\
&L_{15}=-(s_5-s_{18}c_1+s_{11}-s_{26}c_1)\beta\frac{d}{dX}\\
&L_{21}=(s_{10}+s_2)\beta\frac{d}{dX},\qquad L_{22}=s_{10}\frac{d^2}{dX^2}-s_3\beta^2+\lambda^2\\
&L_{23}=-(2s_{26}c_1+s_{18}c_1)\beta\frac{d^2}{dX^2}+s_{19}c_1\beta^3\\
&L_{24}=(s_{11}-s_{26}c_1+s_5-s_{18}c_1)\beta\frac{d}{dX}\\
&L_{25}=(s_{11}-s_{26}c_1)\frac{d^2}{dX^2}-(s_6-s_{19}c_1)\beta^2\\
&L_{31}=s_{17}c_1\frac{d^3}{dX^3}-(2s_{26}c_1+s_{18}c_1)\beta^2\frac{d}{dX}\\
&L_{32}=-(s_{18}c_1+2s_{26}c_1)\beta\frac{d^2}{dX^2}+s_{19}c_1\beta^3\\
&L_{33}=-s_{23}c_1^2\frac{d^4}{dX^4}+(2s_{24}c_1^2\beta^2+4s_{28}c_1^2\beta^2)\frac{d^2}{dX^2}\\
&+(s_{14}-2s_{30}c_2+s_{32}c_2^2)\frac{d^2}{dX^2}-c_1^2\lambda^2p_3\frac{d^2}{dX^2}\\
&-(s_{25}c_1^2\beta^4+s_{13}\beta^2-2s_{29}c_2\beta^2+s_{31}c_2^2\beta^2)\\
&+(\lambda^2+c_1^2\lambda^2p_3\beta^2),\\
&L_{34}=(s_{20}c_1-s_{23}c_1^2)\frac{d^3}{dX^3}-2s_{27}c_1\beta^2\frac{d}{dX}\\
&+(-2s_{28}c_1^2\beta^2+s_{21}c_1\beta^2-s_{24}c_1^2\beta^2)\frac{d}{dX}\\
&+(-s_{14}+2s_{30}c_2-s_{32}c_2^2)\frac{d}{dX}\\
&+(c_1\lambda^2p_2-c_1^2\lambda^2p_3)\frac{d}{dX}\\
&L_{35}=-(s_{21}c_1-s_{24}c_1^2+2s_{27}c_1-2s_{28}c_1^2)\beta\frac{d^2}{dX^2}\\
&+(s_{22}c_1\beta^3-s_{25}c_1^2\beta^3-s_{13}\beta+2s_{29}c_2\beta-s_{31}c_2^2\beta)\\
&-(c_1\lambda^2p_2\beta-c_1^2\lambda^2p_3\beta)\\
&L_{41}=(s_4-s_{17}c_1)\frac{d^2}{dX^2}-(s_{11}-s_{26}c_1)\beta^2
\end{aligned} \tag{12}$$

$$
\begin{aligned}
L_{42} &= -\left(s_5 - s_{18} c_1 + s_{11} - s_{26} c_1 \right) \beta \frac{d}{dX} \\
L_{43} &= \left(s_{23} c_1^2 - s_{20} c_1 \right) \frac{d^3}{dX^3} - \left(s_{24} c_1^2 \beta^2 - s_{21} c_1 \beta^2 \right) \frac{d}{dX} \\
&-\left(2 s_{28} c_1^2 \beta^2 - 2 s_{27} c_1 \beta^2 + s_{14} - 2 s_{30} c_2 + s_{32} c_2^2 \right) \frac{d}{dX} \\
&-\left(c_1 \lambda^2 p_2 - c_1^2 \lambda^2 p_3 \right) \frac{d}{dX} \\
L_{44} &= \left(s_7 - 2 s_{20} c_1 + s_{23} c_1^2 \right) \frac{d^2}{dX^2} \\
L_{45} &= -(s_8 - 2 s_{21} c_1 + s_{24} c_1^2 + s_{21} - 2 s_{27} c_1 \\
&\quad + s_{28} c_1^2) \beta \frac{d}{dX} \\
&-\left(s_{12} \beta^2 - 2 s_{27} c_1 \beta^2 \right) \\
&-\left(s_{28} c_1^2 \beta^2 + s_{14} - 2 s_{30} c_2 + s_{32} c_2^2 \right) \\
&+\left(\lambda^2 p_1 - 2 c_1 \lambda^2 p_2 + c_1^2 \lambda^2 p_3 \right) \\
L_{51} &= \left(s_{11} - s_{26} c_1 + s_5 - s_{18} c_1 \right) \beta \frac{d}{dX} \\
L_{52} &= \left(s_{11} - s_{26} c_1 \right) \frac{d^2}{dX^2} - \left(s_6 - s_{19} c_1 \right) \beta^2 \\
L_{53} &= \left(2 s_{28} c_1^2 - 2 s_{27} c_1 + s_{24} c_1^2 - s_{21} c_1 \right) \beta \frac{d^2}{dX^2} \\
&-\left(s_{25} c_1^2 \beta^3 - s_{22} c_1 \beta^3 + s_{13} \beta - 2 s_{29} c_2 \beta + s_{31} c_2^2 \beta \right) \\
&-\left(c_1 \beta \lambda^2 p_2 - c_1^2 \beta \lambda^2 p_3 \right) \\
L_{54} &= \left(s_{12} - 2 s_{27} c_1 + s_{28} c_1^2 + s_8 - 2 s_{21} c_1 + s_{24} c_1^2 \right) \beta \frac{d}{dX} \\
L_{55} &= \left(s_{12} - 2 s_{27} c_1 + s_{28} c_1^2 \right) \frac{d^2}{dX^2} - s_9 \beta^2 \\
&-\left(-2 s_{22} c_1 \beta^2 + s_{25} c_1^2 \beta^2 + s_{13} - 2 s_{29} c_2 + s_{31} c_2^2 \right) \\
&+\left(\lambda^2 p_1 - 2 c_1 \lambda^2 p_2 + c_1^2 \lambda^2 p_3 \right).
\end{aligned}
\tag{12}
$$

where

$$
\lambda^2 = \frac{I_0 \omega^2 a^2}{A_{11}}, \quad p_1 = \frac{I_2}{I_0 a^2},
$$

$$
p_2 = \frac{I_4}{I_0 a^2}, \; p_3 = \frac{I_6}{I_0 a^2}, \qquad \beta = n\pi\phi,
$$

$$
s_2 = \frac{A_{12}}{A_{11}}, \; s_3 = \frac{A_{22}}{A_{11}}, s_4 = \frac{B_{11}}{aA_{11}}, s_5 = \frac{B_{12}}{aA_{11}}, s_6 = \frac{B_{22}}{aA_{11}},
$$

$$
s_7 = \frac{D_{11}}{a^2 A_{11}}, \; s_8 = \frac{D_{12}}{a^2 A_{11}}, \; s_9 = \frac{D_{22}}{a^2 A_{11}},
$$

$$
s_{10} = \frac{A_{66}}{A_{11}}, s_{11} = \frac{B_{66}}{aA_{11}}, s_{12} = \frac{D_{66}}{a^2 A_{11}}, s_{13} = \frac{A_{44}}{A_{11}},
$$

$$
s_{14} = \frac{A_{55}}{A_{11}}, s_{15} = \frac{B_{16}}{aA_{11}}, s_{16} = \frac{B_{26}}{aA_{11}}, s_{17} = \frac{E_{11}}{a^3 A_{11}},
$$

$$
s_{18} = \frac{E_{12}}{a^3 A_{11}}, s_{19} = \frac{E_{22}}{a^3 A_{11}}, s_{20} = \frac{F_{11}}{a^4 A_{11}}, s_{21} = \frac{F_{12}}{a^4 A_{11}},
$$

$$
s_{22} = \frac{F_{22}}{a^4 A_{11}}, s_{23} = \frac{H_{11}}{a^6 A_{11}}, s_{24} = \frac{H_{12}}{a^6 A_{11}}
$$

$$
s_{25} = \frac{H_{22}}{a^6 A_{11}}, s_{26} = \frac{E_{66}}{a^3 A_{11}}, s_{27} = \frac{F_{66}}{a^4 A_{11}}, s_{28} = \frac{H_{66}}{a^6 A_{11}},
$$

$$
s_{29} = \frac{D_{44}}{a^2 A_{11}}, s_{30} = \frac{D_{55}}{a^2 A_{11}}, s_{31} = \frac{F_{44}}{a^4 A_{11}},
$$

$$
s_{32} = \frac{F_{55}}{a^4 A_{11}}, s_{33} = \frac{E_{16}}{a^3 A_{11}}, s_{34} = \frac{E_{26}}{a^3 A_{11}}, s_{35} = \frac{F_{16}}{a^4 A_{11}},
$$

$$
s_{36} = \frac{F_{26}}{a^4 A_{11}}, s_{37} = \frac{H_{16}}{a^6 A_{11}}, s_{38} = \frac{H_{26}}{a^6 A_{11}}.
$$

2.3 Method of solution

The differential equations in Eq. (11) contains derivative of third order in $U(X)$, second order in $V(X)$, fourth order in $W(X)$, third order in $\Phi_X(X)$ and second order in $\Phi_Y(X)$. These functions are approximated by using cubic and quantic spline functions in the range of $X \varepsilon [0, 1]$, since splines are relatively simple and elegant (Viswanathan and Javed 2016).

The displacement functions $U(X)$, $V(X)$, and $W(X)$and the rotational functions $\Phi_X(X)$, $\Phi_Y(X)$ are approximated respectively by the splines

$$
\begin{aligned}
U(X) &= \sum_{i=0}^{4} a_i X^i + \sum_{j=0}^{N-1} b_j (X - X_j)^5 H(X - X_j) \\
V(X) &= \sum_{i=0}^{2} c_i X^i + \sum_{j=0}^{N-1} d_j (X - X_j)^3 H(X - X_j) \\
W(X) &= \sum_{i=0}^{4} e_i X^i + \sum_{j=0}^{N-1} f_j (X - X_j)^5 H(X - X_j) \\
\Phi_X(X) &= \sum_{i=0}^{4} g_i X^i + \sum_{j=0}^{N-1} g_j (X - X_j)^5 H(X - X_j) \\
\Phi_Y(X) &= \sum_{i=0}^{2} l_i X^i + \sum_{j=0}^{N-1} q_j (X - X_j)^3 H(X - X_j)
\end{aligned}
\tag{13}
$$

Here $H(X - X_j)$ is the Heaviside step function and N is the number of intervals into which the range [0, 1] of X is divided. The points $X = X_s = \frac{s}{N}$, (s = 0, 1, 2,...., N) are chosen as the knots of the splines, as well as the collocation points. Thus the splines are assumed to satisfy the differential equations given by Eq. (11), at all X_s. The resulting expressions contain ($5N$ + 5) homogeneous system of equations in the ($5N$ = 21) spline coefficients.

The boundary condition considered on the edges x = 0 and x = a are; (1) (S-S): both the ends simply supported. This boundary condition gives 13 more equations, thus making a total of ($5N$ + 18) equations, in the same number of unknowns. The resulting field and boundary condition equations may be written in the form

$$
[\, M \,]\{\, q \,\} = \lambda^2 [\, P \,]\{\, q \,\} \tag{14}
$$

where $[M]$ and $[P]$ are square matrices, $\{q\}$ is a column matrix. This is treated as a generalized eigenvalue problem in the eigen parameter λ and the eigenvector $\{q\}$ whose elements are the spline coefficients.

3. Results and discussion

The higher order shear deformation theory is used to investigate the free vibration of cross-ply plates for simply supported boundary conditions. All numerical computations in this section, unless otherwise stated, three materials are considered: Kevlar-49/epoxy (KE), Graphite/Epoxy (AS4/ 3501-6) (GE) and E-glass epoxy (EGE). Symmetric and anti-symmetric plates are considered with two, three, four, five and six layeres accordingly.

3.1 Convergence study

In this subsection the frequency parameter with respect to different parameter values are carried out to confirm the convergence of the spline method for cross-ply plates. The number of subintervals N of the range $X \in [0, 1]$. The value of N started from 4 and finally it is fixed for $N = 18$, since for the next value of N, the percent changes in the values of λ are very low, the maximum being 3%.

3.2 Validation

The validation of the applicability and accuracy of the present results with the available results is shown in Table 1, which is the reduced case of the present study and compared to Srinivas and Rao (1970) (used exact method), Reddy and Phan (1985) (using classical plate theory), Reddy and Phan (1985) (using higher-order shear deformation theory), Nayak *et al*. (2002) (using higher-order shear deformation theory). The material properties are assumed to be: E_1 = 143.53 GPa, E_2 = 75.38 GPa, G_{12} = 42.03 GPa, G_{13} = 25.56 GPa, G_{23} = 42.65 GPa, v_{12} = 0.44. The elastic constant C_{11} = 159.85 GPa. The present results are close to the available results obtained by Srinivas and Rao (1970), Reddy and Phan (1985) and Nayak *et al*. (2002).

3.3 Effect of different materials and geometric parameters on frequencyparameter of the plate

3.3.1 Effect of side-to-thickness ratio

Tables 2 and 3 show the effect of side-to-thickness ratio on fundamental frequency parameter of layered anti-symmetric cross-ply plates. Table 2 shows the variations of the fundamental frequency parameter value for two, four and six layered anti-symmetric cross-ply plates using Graphite/Epoxy (AS4/3501-6) (GE) material for S-S boundary condition. It shows that the fundamental frequency parameter value decreases with the increase of side-to-thickness ratio, whereas the frequency parameter value increases with the increase of number of layers. In Table 3, the effect of different material combinations of six layered plates on the fundamental frequency is shown. It is seen that plates with KE/GE/GE/GE/GE/KE material combination shows the lowest frequency parameter value and the plates with GE/KE/EGE/EGE/KE/GE material combination shows the highest frequency parameter value.

Table 1 Comparison of non-dimensional frequencies $\bar{\Omega} = \Omega h\sqrt{\rho/C_{11}}$ of a simply supported square plate with a/h = 10. Results are compared with Srinivas and Rao (1970), Reddy and Phan (1985) and Nayak *et al*. (2002)

Modes	Exact (Srinivas and Rao 1970)	CPT (Reddy and Phan 1985)	HSDT (Reddy and Phan 1985)	HSDT (Nayak *et al*. 2002)	Present
(1,1)	0.0474	0.0493	0.0474	0.0476	0.0475
(2,1)	0.1188	0.1327	0.1189	0.1205	0.1195
(3,1)	0.2180	0.2671	0.2184	0.2253	0.2190

*Material properties are: E_1 = 143.52 GPa, E_2 = 75.38 GPa, G_{12} = 42.03 GPa, G_{13} = 25.56 GPa, G_{23} = 42.65 GPa, v_{12} = 0.44

Table 2 The fundamental frequencies with side-to-thickness ratio of six- four- and two-layered anti-symmetric cross ply plates: a/b = 1

a/h	λ		
	0°/90°/0°/90°/ 0°/90° GE/GE/GE/GE/GE/GE	0°/90°/0°/90° GE/GE/GE/GE	0°/90° GE/GE
10	0.367043	0.352020	0.274490
20	0.203067	0.197248	0.144321
30	0.137276	0.130948	0.098687
40	0.103302	0.102759	0.074184
50	0.082760	0.079966	0.059599
60	0.069778	0.066635	0.049830

Table 3 The fundamental frequencies with side-to-thickness ratio of six-layered anti symmetric cross ply plates: a/b = 1

a/h	λ				
	0°/90°/0°/90°/ 0°/90°				
	KE/GE/ GE/GE/ GE/KE	KE/GE/ EGE/EGE/ GE/KE	GE/KE/ EGE/EGE/ KE/GE	GE/KE/ KE/E/KE /GE	GE
10	0.346872	0.397367	0.408492	0.367507	0.367043
20	0.186794	0.214416	0.22556	0.20964	0.203067
30	0.12672	0.144213	0.151623	0.140431	0.137276
40	0.096297	0.11013	0.11471	0.10611	0.103302
50	0.077924	0.087891	0.091322	0.086357	0.08276
60	0.06175	0.071584	0.07635	0.07434	0.069778

Figs. 1(a)-(d) describes the effect of side-to-thickness ratio ($10 \le a/h \le 60$) of the plates on the behaviour of frequency parameters (λ_m, m = 1, 2, 3). The different number of layers with anti-symmetric cross ply orientation is considered using the material GE. The aspect ratio (a/b = 1) is fixed. From the figures, it is seen that the frequency parameter value decreases with increasing the side-to-thickness ratio. Further, decrease is fast between $10 \le a/h \le 30$ and becomes slow afterwards. Moreover, the value of the

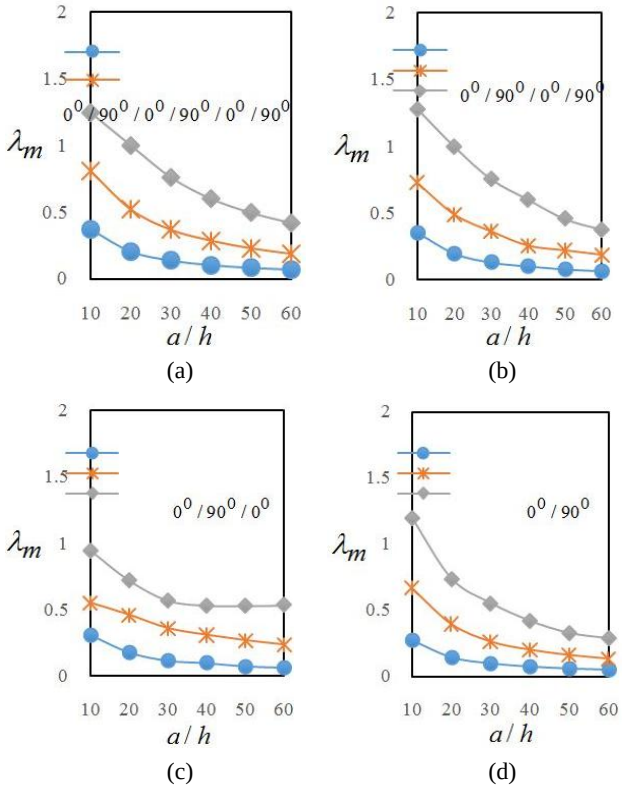

Fig. 1 Variation of frequency parameter with respect to side to thickness ratio of anti-symmetric layered plates with different number of layer of GE material and $a/b = 1$

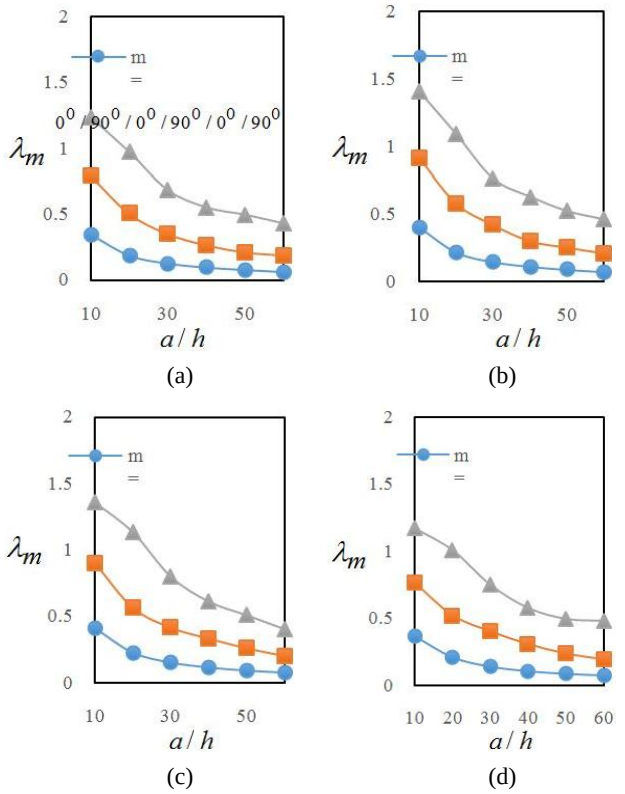

Fig. 2 Variation of frequency parameter with respect to side to thickness ratio of anti-symmetric six layered plates with $a/b = 1$

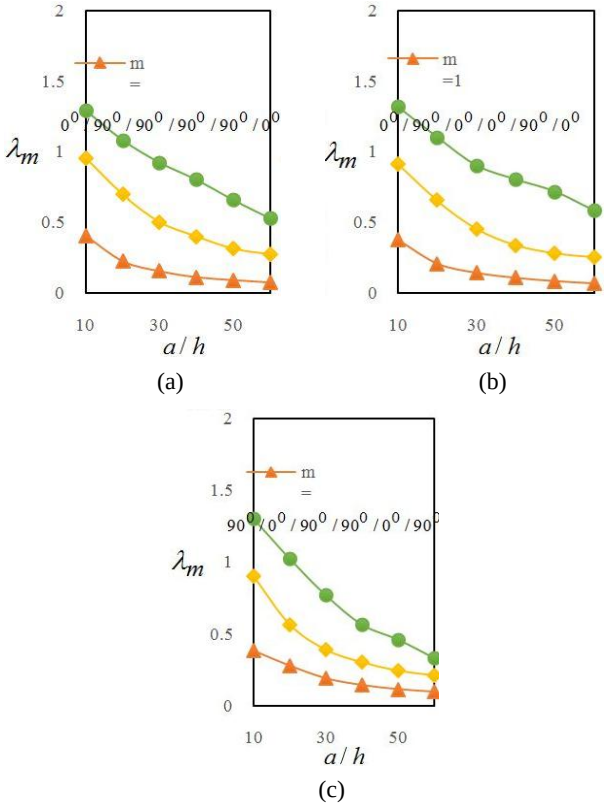

Fig. 3 Variation of frequency parameter with respect to side to thickness ratio of symmetric six layered plates with $a/b = 1$

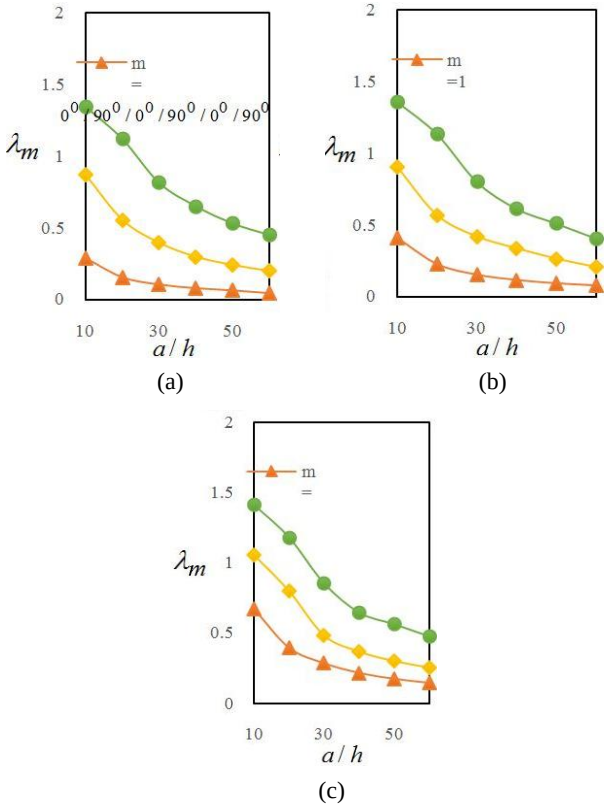

Fig. 4 Variation of frequency parameter with respect to side to thickness ratio of anti-symmetric six layered plates with: (a) $a/b = 0.4$; (b) $a/b = 1$; (c) $a/b = 1.6$

frequency parameter increases as the number of layers and as well as mode number increases.

Effect of the different material combinations of six layered plates between the side-to-thickness ratio and frequency parameter is presented in Figs. 2(a)-(d). The frequency parameter value varies for different material combinations, reveals that the combination of GE, KE and EGE arranged in the order as GE/KE/EGE/EGE/KE/GE in Fig. 2(a) gives higher frequency values as compared to the materials arranged in the orders KE/GE/EGE/EGE/GE/KE, GE/KE/KE/KE/KE/GE and KE/GE/GE/GE/GE/KE shown in Figs. 2(b), (c) and (d) respectively.

The variation of frequency parameter for three different ply orientations with anti-symmetric and symmetric manner having material combination of GE/KE/EGE/EGE/KE/GE are shown in Figs. 3(a)-(c). Generally the frequency parameter value decrease as the side-to-thickness ratio increases.

The decrease is strict between $10 \leq a/h \leq 30$ and slow afterwards. Moreover, the frequency parameter value varies by using different combination of cross-ply angles.

Six layered plates of lamination scheme 0°/90°/0°/90°/0°/90° with the materials arranged as (GE/KE/EGE/EGE/KE/GE) are considered to study the effect of side-to-thickness ratio on the frequency parameter value by fixing aspect ratio a/b = 0.4, 1, 1.6 shown in Figs. 4(a)-(c). It is seen that the value of side-to-thickness ratio increases while the value of the frequency parameter decreases. Moreover, the frequency parameter value increases as aspect ratio increases. The variation of frequency parameter value with respect to the side-to-thickness ratio are shown in Figs. 5(a)-(c) for two layered plates having GE material by fixing the aspect ratio a/b. It is concluded that frequency parameter value is highest for a/b = 1.6 followed by a/b = 1 and a/b = 0.4.

Fig. 6 demonstrates the effect of frequency parameter on side-to-thickness ratio by fixing the aspect ratio as a/b = 0.4, 1, 1.6 for four layered cross ply plates. It is seen that the frequency parameter value decreases as the side-to-thickness ratio increases, whereas the value of frequency parameter increases with the increase of aspect ratio.

The effect of different material combinations and aspect ratio on the fundamental frequency value is studied in Fig. 7 for four layered cross-ply plates. KE/GE/GE/KE, GE/KE/KE/GE and KE/EGE/EGE/KE material combinations are used in Figs. 7(a)-(c) respectively. The figures show that frequency increases with the increase of aspect ratio, but differs marginally by using different material combinations.

The variation of frequency parameter values with respect to side-to-thickness ratio and different material combinations for five layered plates are depicted in Fig. 8. The aspect ratio is fixed a/b = 1. Results concluded that the frequency parameter values for the lamination materials arranged in the order as GE/KE/EGE/KE/GE, KE/GE/EGE/GE/KE and EGE/GE/KE/GE/EGE.

Fig. 9 demonstrates the different combination of lamination materials effecting the frequency parameter value with the increase of side-to-thickness ratio of three layered plates. Figs. 9(a)-(c) exhibits that the value of frequency parameter for lamination arranged in the order as GE/EGE/GE, EGE/KE/EGE and EGE/GE/EGE.

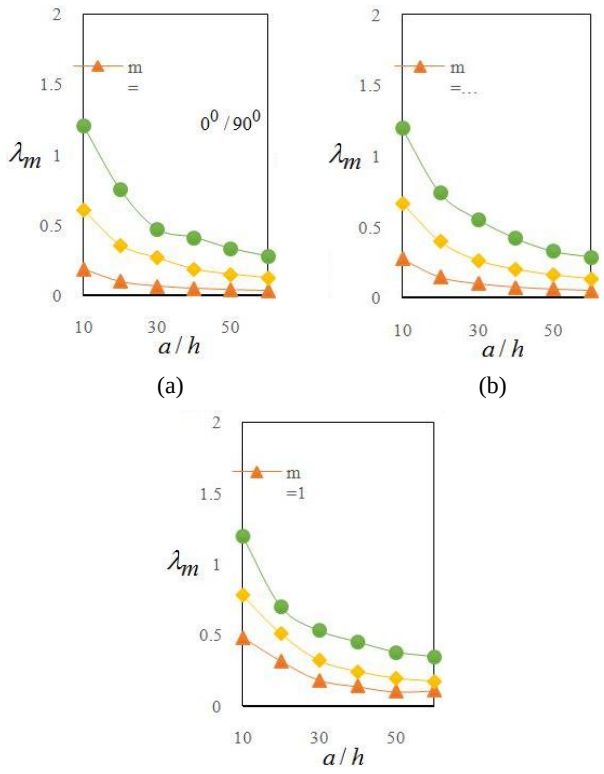

Fig. 5 Variation of frequency parameter with respect to side to thickness ratio of anti-symmetric two layered plates with GE/GE material combinations: (a) a/b = 0.4; (b) a/b = 1; (c) a/b = 1.6

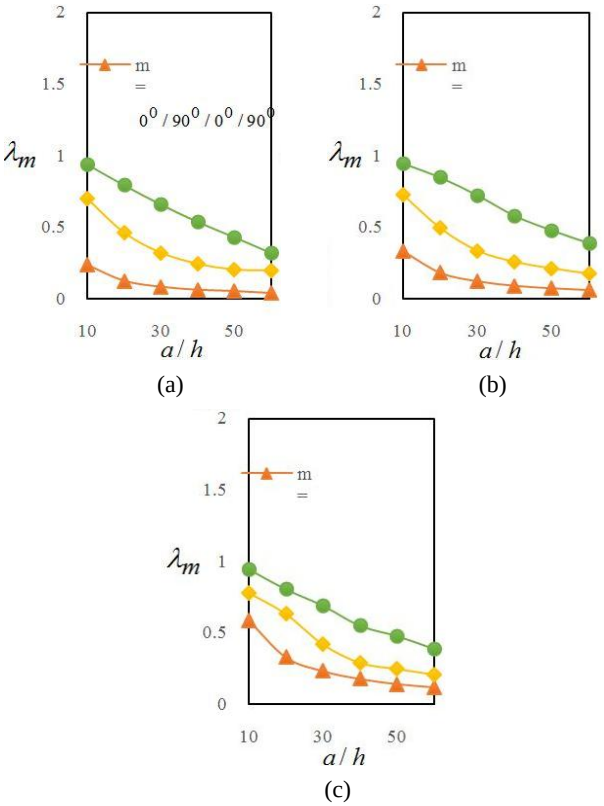

Fig. 6 Variation of frequency parameter with respect to side to thickness ratio of anti-symmetric four layered plates with: (a) a/b = 0.4; (b) a/b = 1; (c) a/b = 1.6

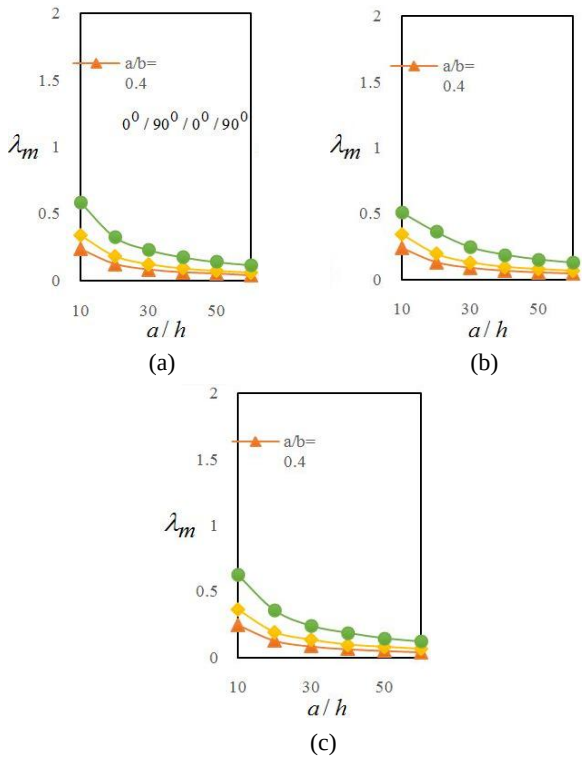

Fig. 7 Fundamental frequency parameter variation with respect to side to thickness ratio of anti-symmetric four layered plates with: (a) KE/GE/ GE/KE; (b) GE/KE/KE/GE; (c) KE/EGE/ EGE/KE material combinations

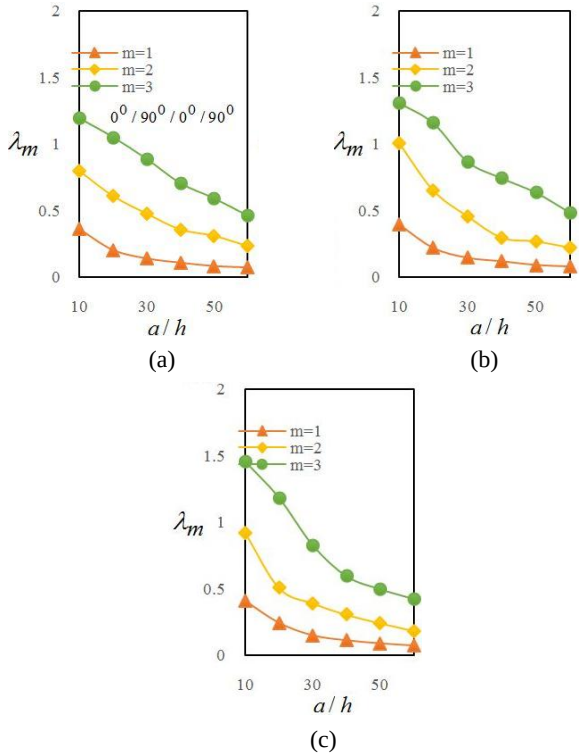

Fig. 8 Variation of frequency parameter with respect to side to thickness ratio of anti-symmetric five layered plates with: (a) GE/KE/EGE/KE/GE; (b) KE/GE/ EGE/GE/KE; (c) EGE/GE/KE/GE/EGE material combinations and a/b=1

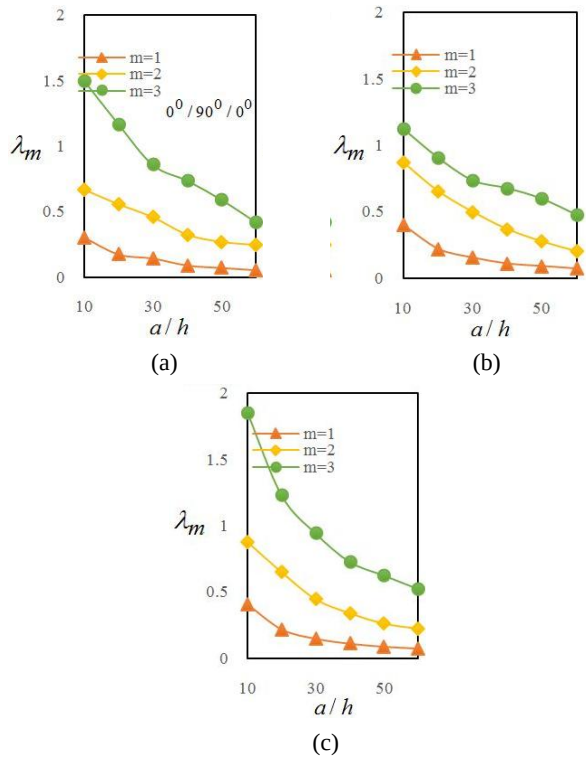

Fig. 9 Variation of frequency parameter with respect to side to thickness ratio of anti-symmetric three layered plates with: (a) GE/EGE/GE; (b) EGE/KE/EGE; (c) EGE/GE/EGE material combinations and $a/b = 1$

3.3.2 Effect of side-to-thickness ratio

The effect of number of layers and different material combination are studied on fundamental frequency parameter with respect to the aspect ratio and shown in Tables 4 and 5. In Table 4, it is seen that the frequency value in increases with the increase of aspect ratio and number of layers. In Table 5 frequency of five layered plates with different material sequences are shown. It

Table 4 The fundamental frequencies with aspect ratio of layered anti-symmetric cross ply plates: $a/h = 10$

a/b	λ				
	0°/90° (GE/GE)	0°/90°/0° (GE/KE/ GE)	0°/90°/ 0°/90°/0° (GE/KE/ KE/GE)	0°/90°/0°/ 90°/0° (GE/KE/ EGE/KE/GE)	0°/90°/0°/ 90°/0°/90° (GE/KE/KE/ KE/KE/GE)
0.2	0.177784	0.262125	0.235697	0.316345	0.242200
0.4	0.185269	0.265360	0.242493	0.323357	0.258542
0.6	0.200550	0.268430	0.260049	0.322310	0.276981
0.8	0.231146	0.274075	0.296675	0.337451	0.313034
1.0	0.274706	0.294306	0.345316	0.361345	0.367861
1.2	0.336994	0.304561	0.408997	0.397780	0.436413
1.4	0.438473	0.327727	0.482600	0.444140	0.517420
1.6	0.476875	0.351892	0.544230	0.481529	0.616116
1.8	0.562218	0.468920	0.627314	0.559093	0.670023
2.0	0.660780	0.521389	0.703584	0.586980	0.774660

Table 5 The fundamental frequencies with aspect ratio of five layered anti-symmetric cross ply plates: a/h = 10

a/b	λ				
	0°/90°/0°/90°/0°				
	(EGE/EGE/EGE/EGE/EGE)	(KE/GE/EGE/GE/KE)	(GE/KE/KE/KE/GE)	(GE/KE/EGE/KE/GE)	(EGE/GE/KE/GE/EKE)
0.2	0.302881	0.313278	0.279410	0.316345	0.253083
0.4	0.303214	0.320993	0.282251	0.323357	0.278370
0.6	0.330603	0.334741	0.289731	0.322310	0.298500
0.8	0.358871	0.359871	0.301851	0.337451	0.321948
1.0	0.420726	0.419306	0.326710	0.361345	0.408806
1.2	0.486287	0.463769	0.361000	0.397780	0.485093
1.4	0.534112	0.537924	0.402441	0.444140	0.588901
1.6	0.665426	0.661241	0.451081	0.481529	0.681860
1.8	0.761771	0.717251	0.506165	0.559093	0.802595
2.0	0.878293	0.812177	0.517710	0.586980	0.956563

provides that the five layered plates with the material combination of EGE/GE/KE/GE/EGE shows the lowest frequency values and GE/KE/EGE/KE/GE and KE/GE/EGE/GE/KE material sequence shows the higher frequency values.

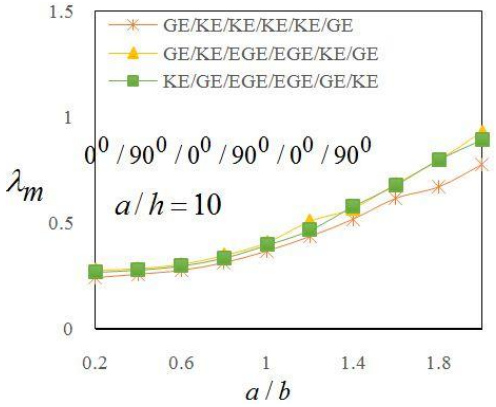

Fig. 10 Fundamental frequency parameter variation with respect to aspect ratio of anti-symmetric six layered plates

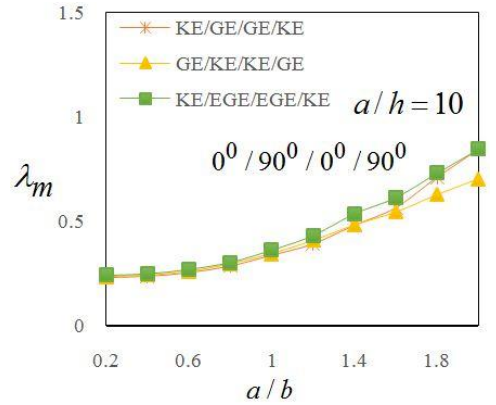

Fig. 11 Fundamental frequency parameter variation with respect to aspect ratio of anti-symmetric four layered plates

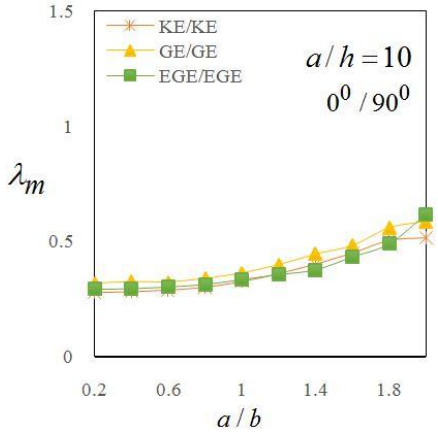

Fig. 12 Fundamental frequency parameter variation with respect to aspect ratio of anti-symmetric two layered plates

Fig. 11 depicts the anti-symmetric four layered plates with the influence of different lamination material combinations and aspect ratio under S-S boundary conditions and a/b = 10 is fixed. It is seen that there is negligible difference in the value of fundamental frequency between 0.2 < a/b < 1 and difference slightly increases afterwards.

Two layered plates of different lamination materials are used to observe the effect of aspect ratio on the fundamental frequency in Fig. 12. From the figure, it shows that the fundamental frequency value increases slowly with the increase of aspect ratio. Further, the lamination material slightly effects the value of fundamental frequency.

Figs. 13 and 14 show the effect of three and five layered anti-symmetric plates on the fundamental frequency. The characterise pattern of the curves are similar for both the graphs. The EGE/GE/EGE, GE/KE/GE and EGE/KE/EGE material combinations are used in Fig. 13 and GE/KE/KE/KE/GE, GE/KE/EGE/KE/GE and GE/EGE/KE/EGE/KE material combinations are used in Fig. 14. There is a slow increase in the value of fundamental frequency with respect to aspect ratio in both the figures. Moreover, the funda-

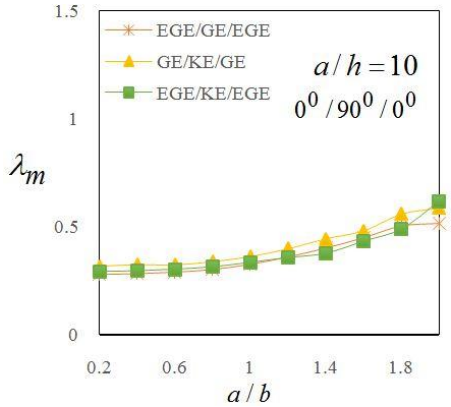

Fig. 13 Fundamental frequency parameter variation with respect to aspect ratio of anti- symmetric three layered plates

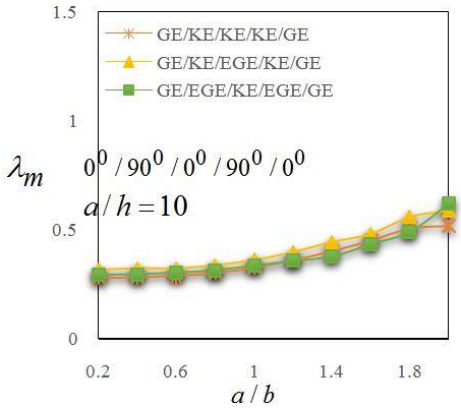

Fig. 14 Fundamental frequency parameter variation with respect to aspect ratio of anti-symmetric five layered plates with GE/KE/KE/KE/GE, GE/KE/EGE/KE/GE, and GE/EGE/KE/EGE/GE material combinations

mental frequency value slightly differs while using the different material combinations.

4. Conclusions

The present study investigates the free vibration of anti-symmetric and symmetric cross-ply plates using cubic and quintic splines under higher-order shear deformation theory. The vibrational behaviour of laminated plates are analysed for simply-supported boundary conditions. The vibration characteristic of the plates is presented for side-to-thickness ratio, aspect ratio, different number of layers, stacking sequence and three different lamination materials. It is concluded that the variation of the geometric parameters and materials combination effects the frequency and the effect is more significant. The applicability and accuracy of the present results with the available results validates that current results may be valuable for the engineers of related fields.

Acknowledgments

This work was supported by Post doctoral Research program under Research Management Centre (RMC), Universiti Teknologi Malaysia, Johor Bahru, Johor, Malaysia and Special Education Program for Offshore Plant under the Ministry of Trade, Industry and Energy affairs (MOTIE), South Korea.

References

Bai, E. and Chen, A. (2013), "A symplecticeigenfunction expansion approach for free vibration solutions of rectangular Kirchhoff plates", *J. Vib. Control*, **19**(8), 1208-1215.

Cho, M. and Parmerter, R. (1993), "Efficient higher order composite plate theory for general lamination configurations", *AIAA Journal*, **31**(7), 1299-1306.

Ferreira, A., Roque, C. and Martins, P. (2003), "Analysis of composite plates using higher-order shear deformation theory and a finite point formulation based on the multiquadric radial basis function method", *Compos. Part B: Eng.*, **34**(7), 627-636.

Groh, R. and Weaver, P. (2015), "Static inconsistencies in certain axiomatic higher-order shear deformation theories for beams, plates and shells", *Compos. Struct.*, **120**, 231-245.

Iurlaro, L., Gherlone, M. and Di Sciuva, M. (2015), "The (3, 2)-mixed refined zigzag theory for generally laminated beams: theoretical development and C0 finite element formulation", *Int. J. Solids Struct.*, **73**, 1-19.

Javed, S., Viswanathan, K.K., Aziz, Z.A. and Prabakar, K. (2016), "Free vibration of anti-symmetric angle-ply plates with variable thickness", *Compos. Struct.*, **137**, 56-69.

Kant, T. and Swaminathan, K. (2001a), "Analytical solutions for free vibration of laminated composite and sandwich plates based on a higher-order refined theory", *Compos. Struct.*, **53**(1), 73-85.

Kant, T. and Swaminathan, K. (2001b), "Free vibration of isotropic, orthotropic, and multilayer plates based on higher order refined theories", *J. Sound Vib.*, **241**(2), 319-327.

Kant, T. and Swaminathan, K. (2002), "Analytical solutions for the static analysis of laminated composite and sandwich plates based on a higher order refined theory", *Compos. Struct.*, **56**(4), 329-344.

Karttunen, A.T. and von Hertzen, R. (2015), "Exact theory for a linearly elastic interior beam", *Int. J. Solids Struct.*, **78-79**, 125-130.

Khdeir, A. (2001), "Free and forced vibration of antisymmetric angle-ply laminated plate strips in cylindrical bending", *J. Vib. Control*, **7**(6), 781-801.

Lee, C.-Y. (2013), "Zeroth-order shear deformation micro-mechanical model for composite plates with in-plane heterogeneity", *Int. J. Solids Struct.*, **50**(19), 2872-2880.

Mackerle, J. (2002), "Finite element analyses of sandwich structures: a bibliography (1980-2001)", *Eng. Comput.*, **19**(2), 206-245.

Mantari, J.L. and Granados, E.V. (2015), "Thermoelastic analysis of advanced sandwich plates based on a new quasi-3D hybrid type HSDT with 5 unknowns", *Compos. Part B: Eng.*, **69**, 317-334.

Mantari, J.L., Oktem, A.S. and Soares, C.G. (2011), "Static and dynamic analysis of laminated composite and sandwich plates and shells by using a new higher-order shear deformation theory", *Compos. Struct.*, **94**(1), 37-49.

Mantari, J.L., Oktem, A. and Soares, C.G. (2012), "A new higher order shear deformation theory for sandwich and composite laminated plates", *Compos. Part B: Eng.*, **43**(3), 1489-1499.

Matsunaga, H. (2008), "Free vibration and stability of functionally graded plates according to a 2-D higher-order deformation theory", *Compos. Struct.*, **82**(4), 499-512.

Ma'en, S.S. and Butcher, E.A. (2012), "Free vibration analysis of rectangular and annular Mindlin plates with undamaged and damaged boundaries by the spectral collocation method", *J. Vib. Control*, **18**(11), 1722-1736.

Mindlin, R.D. (1951), "Influence of rotatory inertia and shear on flexural motions of isotropic, elastic plates", *ASME J. Appl. Mech.*, **18**, 31-38.

Nayak, A., Moy, S. and Shenoi, R. (2002), "Free vibration analysis of composite sandwich plates based on Reddy's higher-order theory", *Compos. Part B: Eng.*, **33**(7), 505-519.

Neves, A., Ferreira, A., Carrera, E., Cinefra, M., Roque, C., Jorge, R. and Soares, C.G. (2013), "Static, free vibration and buckling analysis of isotropic and sandwich functionally graded plates using a quasi-3D higher-order shear deformation theory and a meshless technique", *Compos. Part B: Eng.*, **44**(1), 657-674.

Nguyen, T.N., Thai, C.H. and Xuan, H.N. (2016), "On the general framework of high order shear deformation theories for laminated composite plate structures: A novel unified approach", *Int. J. Mech. Sci.*, **110**, 242-255.

Nguyen, T.N., Ngo, T.D. and Xuan, H.N. (2017), "A novel three-variable shear deformation plate formulation: Theory and Isogeometric implementation", *Comput. Methods Appl. Mech. Eng.*, **326**, 376-401.

Noor, A.K., Burton, W.S. and Bert, C.W. (1996), "Computational models for sandwich panels and shells", *Appl. Mech. Rev.*, **49**(3), 155-199.

Pai, P.F. (1995), "A new look at shear correction factors and warping functions of anisotropic laminates", *Int. J. Solids Struct.*, **32**(16), 2295-2313.

Pai, P.F. and Schulz, M.J. (1999), "Shear correction factors and an energy-consistent beam theory", *Int. J. Solids Struct.*, **36**(10), 1523-1540.

Peković, O., Stupar, S., Simonović, A., Svorcan, J. and Komarov, D. (2014), "Isogeometric bending analysis of composite plates based on a higher-order shear deformation theory", *J. Mech. Sci. Technol.*, **28**(8), 3153-3162.

Phung-Van, P., Nguyen-Thoi, T., Bui-Xuan, T. and Lieu-Xuan, Q. (2015a), "A cell-based smoothed three-node Mindlin plate element (CS-FEM-MIN3) based on the C0-type higher-order shear deformation for geometrically nonlinear analysis of laminated composite plates", *Computat. Mater. Sci.*, **96**, 549-558.

Phung-Van, P., De Lorenzis, L., Thai, C.H., Abdel-Wahab, M. and Nguyen-Xuan, H. (2015b), "Analysis of laminated composite plates integrated with piezoelectric sensors and actuators using higher-order shear deformation theory and isogeometric finite elements", *Computat. Mater. Sci.*, **96**, 495-505.

Rajagopal, A. and Hodges, D.H. (2015), "Variational asymptotic analysis for plates of variable thickness", *Int. J. Solids Struct.*, **75-76**, 81-87.

Reddy, J.N. (2006), *Theory and Analysis of Elastic Plates and Shells*, (2nd Edition), CRC Press, Boca Raton, FL, USA.

Reddy, J.N. and Phan, N.D. (1985), "Stability and vibration of isotropic, orthotropic and laminated plates according to a higher-order shear deformation theory", *J. Sound Vib.*, **98**(2), 157-170.

Reissner, E. (1945), "The effect of transverse shear deformation on the bending of elastic plates", *ASME J. Appl. Mech.*, **12**, A68-77.

Saha, K., Misra, D., Pohit, G. and Ghosal, S. (2004), "Large amplitude free vibration study of square plates under different boundary conditions through a static analysis", *J. Vib. Control*, **10**(7), 1009-1028.

Sheikh, A.H. and Chakrabarti, A. (2003), "A new plate bending element based on higher-order shear deformation theory for the analysis of composite plates", *Finite Elem. Anal. Des.*, **39**(9), 883-903.

Singh, D.B. and Singh, B.N. (2017), "New higher order shear deformation theories for free vibration and buckling analysis of laminated and braided composite plates", *Int. J. Mech. Sci.*, **131-132**, 265-277.

Srinivas, S. and Rao, A.K. (1970), "Bending vibration and buckling of simply supported thick orthotropic rectangular plates and laminates", *Int. J. Solids Struct.*, **6**(11), 1463-1481.

Thai, C.H., Nguyen-Xuan, H., Bordas, S.P.A., Nguyen-Thanh, N. and Rabczuk, T. (2015), "Isogeometric analysis of laminated composite plates using the higher-order shear deformation theory", *Mech. Adv. Mater. Struct.*, **22**(6), 451-469.

Tran, L.V., Nguyen-Thoi, T., Thai, C.H. and Nguyen-Xuan, H. (2013), "An edge-based smoothed discrete shear gap method using the C0-type higher-order shear deformation theory for analysis of laminated composite plates", *Mech. Adv. Mater. Struct.*, **22**(4), 248-268.

Vinson, J.R. (2001), "Sandwich structures", *Appl. Mech. Rev.*, **54**(3), 201-214.

Viswanathan, K.K. and Javed, S. (2016), "Free vibration of anti-symmetric angle-ply cylindrical shell walls using first-order shear deformation theory", *J. Vib. Control*, **22**(7), 1757-1768. DOI: 10.1177/1077546314544893

Viswanathan, K.K. and Lee, S.K. (2007), "Free vibration of laminated cross-ply plates including shear deformation by spline method", *Int. J. Mech. Sci.*, **49**(3), 352-363.

Viswanathan, K.K., Javed, S., Aziz, Z.A. and Prabakar, K. (2015a), "Free vibration of symmetric angle-ply laminated annular circular plate of variable thickness under shear deformation theory", *Meccanica*, **50**(12), 3013-3027.

Viswanathan, K., Javed, S., Prabakar, K., Aziz, Z.A. and Bakar, I.A. (2015b), "Free vibration of anti-symmetric angle-ply laminated conical shells", *Compos. Struct.*, **122**, 488-495.

Viswanathan, K.K., Aziz, Z.A., Javed, S., Yaacob, Y. and Pullepu, B. (2015c), "Free vibration of symmetric angle ply truncated conical shells under different boundary conditions using spline method", *J. Mech. Sci. Technol.*, **29**(5), 2073-2080.

Yang, P.C., Nooris, C.H. and Stavsky, Y. (1966), "Elastic wave propogation in heterogeneous plates", *Int. J. Solids Struct.*, **2**(4), 665-684.

Yang, H.T., Saigal, S., Masud, A. and Kapania, R. (2000), "A survey of recent shell finite elements", *Int. J. Numer. Methods Eng.*, **47**(1-3), 101-127.

Zhen, W. and Wanji, C. (2006), "Free vibration of laminated composite and sandwich plates using global–local higher-order theory", *J. Sound Vib.*, **298**(1), 333-349.

CC